Anal Bioanal Chem (2011) 399:2711–2718
DOI 10.1007/s00216-010-4155-0

ORIGINAL PAPER

High-resolution, imaging TOF-SIMS: novel applications in medical research

Per Malmberg · Eva Jennische · Daniel Nilsson · Håkan Nygren

Received: 8 June 2010 / Revised: 17 August 2010 / Accepted: 19 August 2010 / Published online: 9 September 2010

Abstract The use of high-resolution, imaging TOF-SIMS is described and examples are made to demonstrate the application of the method in medical research. Cytochemistry by TOF-SIMS is shown by localization of diacylglycerol (DG) in cryostat sections of hyaline cartilage and by localization of corticosterone in cryostat sections of the adrenal gland cortex. Quantitative measurements and comparison of groups is shown by comparing the lipid content of adipose tissue from two mouse strains, transgenic mouse expressing the FOXC2 gene and wild-type controls. Finally, biopsies made for histopathological diagnosis of infantile reversible cytochrome c oxidase deficiency myopathy were analyzed in order to define the chemical content of areas showing a pathological structure in the light microscope. The use of high-resolution, imaging TOF-SIMS in medical research allows analysis of intact tissue and probe-free localization of specific target molecules in cells and tissues. The TOF-SIMS analysis is not dependent on penetration of reagents into the sample and also independent of probe reactivity such as cross-reactivity or background staining. The TOF-SIMS method can be made quantitative and allows for analysis of specific target molecules in defined tissue compartments.

Keywords TOF-SIMS · Cytochemistry · Histopathological diagnosis

This paper was published in the special issue on *Advances in Analytical Mass Spectrometry* with Guest Editor Maria Careri.

P. Malmberg · E. Jennische · H. Nygren
Department of Medical Chemistry and Cell Biology, Institute of Biomedicine, The Sahlgrenska Academy, University of Gothenburg, P.O. Box 100, 405 30 Göteborg, Sweden

D. Nilsson
Department of Medical Genetics, Institute of Biomedicine, The Sahlgrenska Academy, University of Gothenburg, Box 100, 405 30 Göteborg, Sweden

H. Nygren (✉)
Institute of Biomedicine, P.O. Box 420, 405 30 Göteborg, Sweden
e-mail: hakan.nygren@gu.se

Introduction

Time of flight-secondary ion mass spectrometry (TOF-SIMS) is based on the acceleration of high-energy primary ions onto a target. Secondary electrons, neutrals and ions are emitted from the target reflecting its chemical composition, making possible simultaneous analysis and localization of a plethora of target molecules at submicron resolution, information that cannot be obtained with other analytical methods. Although the TOF-SIMS technique has been available since the sixties, analysis of biological samples has been hampered by the extensive fragmentation of the target molecules and low yield of secondary ions. Comprehensive fragmentation of macromolecules obstructs the identification of the molecule of origin since small fragments need not be specific for the macromolecule of origin. The possibility of analyzing biological samples was improved with the advent of primary ion cluster sources [1].The development of this technique has the potential to make TOF-SIMS as important for medical research as the electron microscope or fluorescence microscopy. The TOF-

SIMS technique is now exploited for use in biomedical and medical research [2] and stands as an alternative and complement to other more established methods such as imaging MALDI [3, 4].

At the first analysis of cryostat sections of rat cerebellum with the Bi-cluster primary ion source, a problem was faced when trying to identify all new peaks found in the spectra [5]. In previous works with a Ga primary ion source, it was only possible to identify the cholesterol signal and the secondary ion of the phosphocholine headgroup [6], in contrast, the spectra obtained using the Bi_3^+ ion source contained a multitude of new secondary ion peaks the identity of which had to be defined. The mass resolution and accuracy of the TOF-SIMS instrument is too low to allow identification of the secondary ion peaks from first principles and it was not safe to rely only on identification based on other MS techniques where fragmentation may occur by different mechanisms. The use of reference samples became the method of choice for the continued work with TOF-SIMS analysis of biological samples, allowing peaks to be assigned to reference compounds, while keeping in mind that in tissue other endogenous species can produce isobaric fragment ions which the lower mass resolution of the TOF-SIMS instrument cannot resolve.

The aim of this article is to present original data representing new applications of imaging TOF-SIMS analysis in medical research. The description of the use of the TOF-SIMS technique in medical research is divided into three sections, explorative cytochemistry, comparison of groups and analysis of biopsies made for histopathological diagnosis of myopathies, where the chemical composition of tissue areas showing pathological structural changes can be selected and analyzed as regions of interest (ROI).

Materials and methods

Animals: FOXC2 transgenic mice were created as previously described [7]. Female FOXC2 transgenic and wild-type littermates (~20 weeks of age) were housed under controlled temperature (23 °C) and lighting (12 h of light, 0700–1900; 12 h of dark, 1900–0700) with free access to water and standard mouse chow. Mice were killed by cervical dislocation and intra-abdominal white adipose tissue was dissected out and transferred to saline.

Rats, Sprague–Dawley (250 g), were kept under standard conditions. The animals were anesthesized with isofluorane and sacrificed by opening the heart. The adrenal glands and the trachea and thyroid glands were dissected out and snap frozen.

Tissue preservation: high pressure freezing was performed at 2,000 bar and −196 °C with the EMPACT (Leica, Vienna), as described in detail by others [8]. Small tissue samples of 2 mm in diameter were cut out with a scalpel blade under saline at room temperature. The tissue pieces were placed onto the freeze-fracture carrier under a stereomicroscope and the copper ring was put on top of the loaded carrier. With help of the loading station, the sample was inserted into the instrument. After cryofixation and freeze fracturing by removing the copper ring, the carriers were collected in the liquid nitrogen bath of the EMPACT and transferred to a brass block, chilled with LN_2. Freeze drying was performed at 10^{-3} mbar for 48 h. The freeze-dried samples were stored in an exsiccator until analyzed by TOF-SIMS within 48 h. Samples with a large plane fractured area were selected for TOF-SIMS analysis in order to minimize topographical effects on the analysis.

Cryostat sectioning: the samples were cut in tissue blocks of about 3–4 mm in diameter and directly plunge frozen in liquid nitrogen. The frozen tissue was cut with a Leica cryostat at -20 °C in slices of 8 μm thickness. The slices were placed onto an object slide and dried at room temperature. Until measurement with TOF-SIMS, the samples were kept dry in a desiccator.

Cryostat sectioned samples of muscle biopsies from patients suffering from reversible cytochrome c oxidase deficiency myopathy [9] were obtained from Professor Anders Oldfors, Department of Pathology, Institute of Biomedicine, University of Gothenburg.

TOF-SIMS analysis: tissue biopsies were analyzed using a TOF-SIMS V instrument (ION-TOF, GmbH, Münster, Germany) equipped with a Bi_3^+-liquid metal ion gun [10] at the University of Gothenburg. The bunched mode (mass resolution $m/\Delta m$, 5000; focus of the ion beam, 3 μm) [11] with a target current of 0.15 pA was used to acquire high mass resolution images of the high pressure frozen fat biopsies at areas ranging from 500×500 μm^2 to 250×250 μm^2.

All image analysis were performed using the ION-TOF Ion image software (Version 4.1, ION-TOF, GmbH, Münster, Germany) except for image resizing, for publication purposes, which was done in Adobe Photoshop CS-2 (Adobe Systems Incorporated, San Jose, CA). Each ion image is normalized to the intensity in the brightest pixel. This intensity value is assigned to the color value of 256. Zero intensity is assigned to the color value 0. All other intensities are assigned accordingly using a linear relationship.

Quantitative analysis of mass spectra was performed by calculating the corrected intensity (Poisson-corrected summed intensity of the peak area) for each peak of interest in several spectra from each tissue biopsy type. The corrected peak intensity was normalized to the total ion count for each spectrum and the data was analyzed in Microsoft Office Excel 2007. The data were analyzed with Student's unpaired t test. Values are presented as

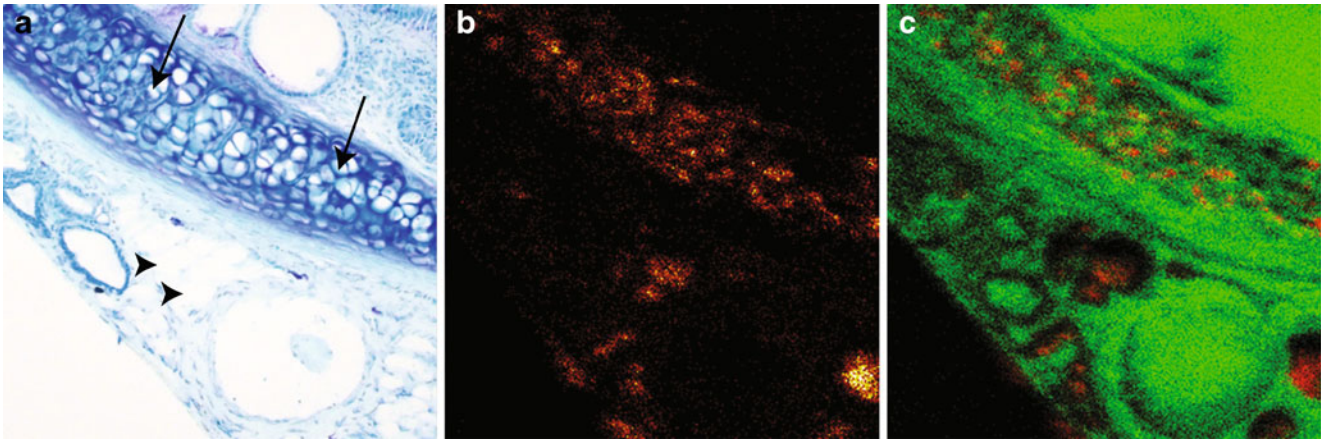

Fig. 1 Cryostat section of rat trachea, dried at room temperature. **a** Light micrograph of cryostat section stained with methylene blue. Hyaline cartilage (*arrows*) can be seen together with scattered adipocytes (*arrowheads*), tracheal glands and a peripheral part of the thyroid gland. Image size 500×500 μm. **b** TOF-SIMS ion image showing the distribution of diacylglycerol (*m/z* 551 and 577). High secondary ion signal is seen in adipocytes and chondrocytes. **c** An overlay TOF-SIMS image with phosphocholine (*m/z* 184) in green and diacylglycerol (*m/z* 551 and 577) in red

means±S.D. A *p* value less than 0.05 were considered statistically significant. Principal component analysis (PCA) was performed in PASW Statistics 18 (SPSS. Inc). Briefly peak intensity data from 47 of the most abundant peaks detected in spectra from TG and wild-type mouse white adipose tissue was analyzed. Principal components were extracted and displayed using Varimax rotation.

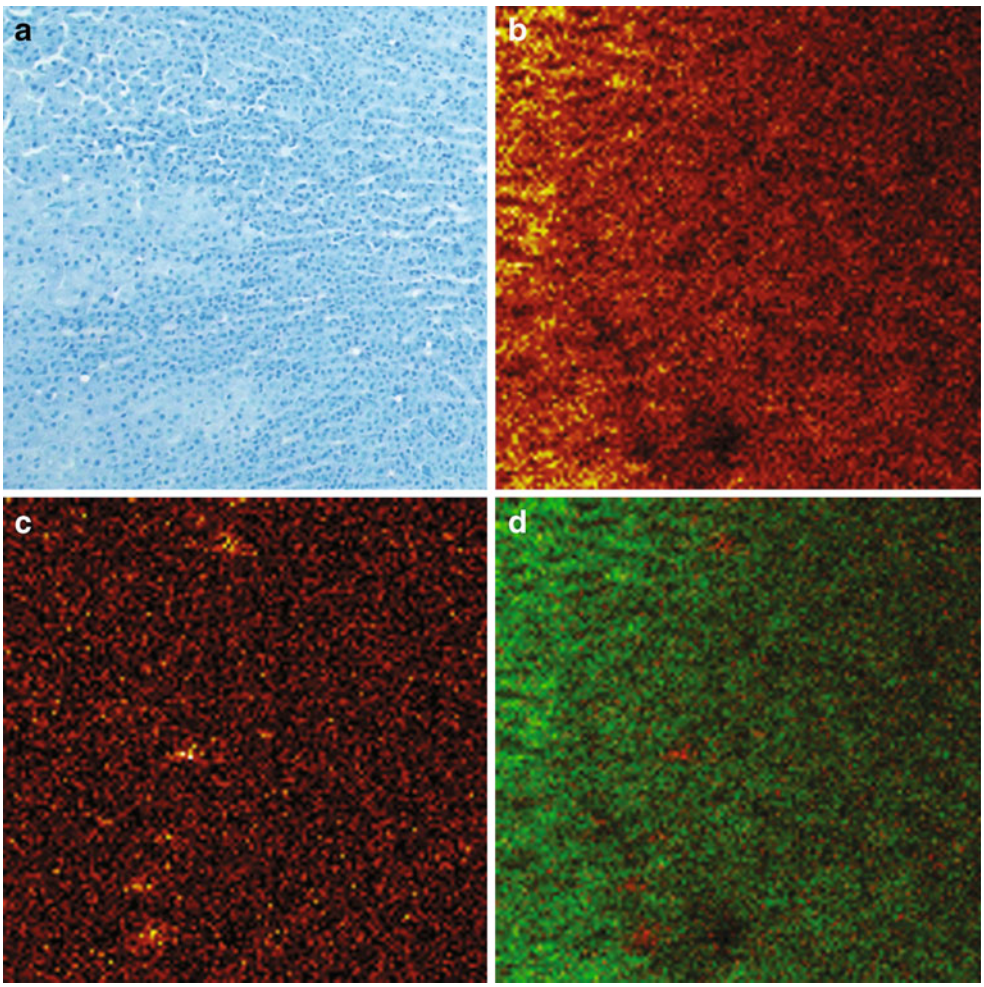

Fig. 2 Cryostat section of a rat adrenal gland. **a** Light microscopy image of a cryostat section stained with methylene blue. Image size 500×500 μm, indicating the regions analyzed in **b-d**. The zona glomerulosa and zona fasciculata of the adrenal cortex are seen. **b** TOF-SIMS ion image showing the distribution of cholesterol (*m/z* 369) in the analyzed adrenal gland cryostat section. Image size 500×500 μm. The original 256×256 pixel images have been down-sampled to 128×128 pixels to increase image intensity, resulting in a image pixel resolution of approx 4 μm/pixel. **c** TOF-SIMS ion image showing the distribution of corticosterone (*m/z* 347). Image size 500×500 μm and image resolution 128×128 pixels. **d** Overlay mage of corticosterone (*m/z* 347) in red and cholesterol (*m/z* 369) in green, mixing of channels will be shown as yellow

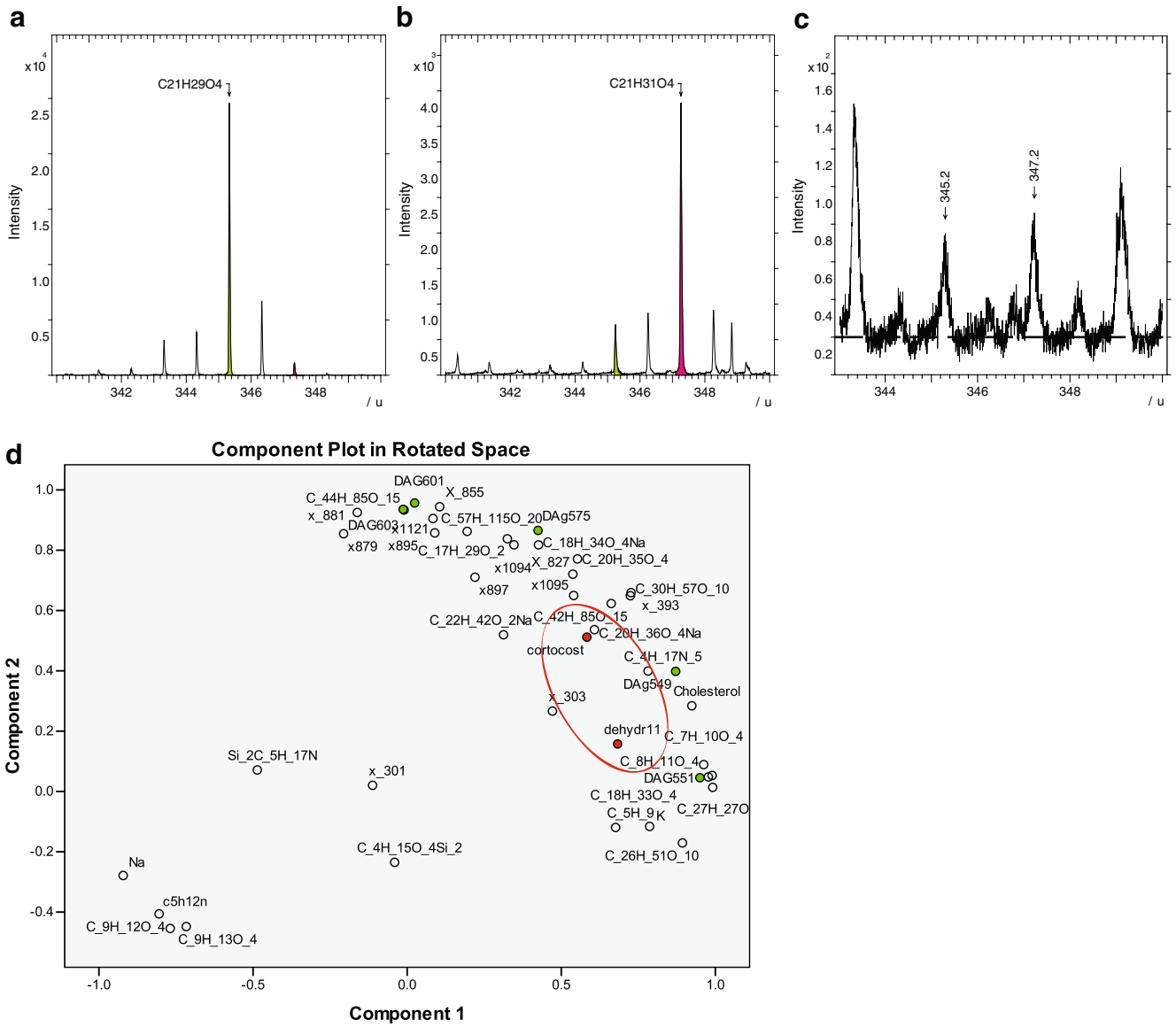

Fig. 3 TOF-SIMS analysis of 11-dehydrocorticosterone and corticosterone in mouse adipose tissue. **a** Shows the reference spectrum from 11-dehydrocorticosterone, $C_{21}H_{29}O_4$ (*m*/*z* 345) and **b** shows the reference spectrum from corticosterone $C_{21}H_{31}O_4$ (*m*/*z* 347). **c** Shows a spectrum from mouse adipose tissue indicating the presence of 11-dehydrocorticosterone and corticosterone together with the estimated noise level (*bar*). **d** Shows a component plot from a principal component analysis of 47 different peaks in mass spectra from mouse adipose tissue. *Red dots* mark the influence of 11-dehydrocorticosterone and corticosterone on the PCA model. *Green dots* show the influence of different diacylglycerol species

Results

Cytochemistry

Figure 1 shows a cryosection of the tracheal wall. The light microscopy image, stained with methykene blue (Fig. 1a), shows hyaline cartilage (arrow), adipocytes (arrowheads) a blood vessel, part of the thyroid gland and tracheal glands in the luminal connective tissue. The TOF-SIMS images show the distribution of the diacylglycerol secondary ion signal (DG, Fig. 1b) and an overlay of DG and the phosphocholine signal (Fig. 1c). The distribution of the DG signal reveals an accumulation of lipids in the chondrocytes of the hyaline cartilage.

Figure 2 shows a cryosection of the adrenal gland cortex, with the zona glomerulosa and zona fasciculata (Fig. 2a). Adrenal cortex cells can be seen in rows. A concentration gradient of the cholesterol signal (*m*/*z* 369, Fig. 2b) is seen from the zona glomerulosa and some cells show corticosterone secondary ion signal (*m*/*z* 347, Fig. 2c). An overlay of the corticosterone signal and the cholesterol signal is shown in Fig. 2d.

Table 1 Identified ions from positive and negative ion mode spectra with measured intensity values and deviations from calculated mass values

Ion mode	Possible lipid species/ molecules	Molecular formula	Measured *m/z*	Calculated *m/z*	Δ*m/z* (ppm
Positive					
	11-Dehydrocorticosterone	$C_{21}H_{29}O_4$	345.19	345.21	−39.7
	Corticosterone	$C_{21}H_{31}O_4$	347.24	347.22	39.5
	DG(32:0)	$C_{35}H_{67}O_4$	551.48	551.5	−39.8
	DG(34:1)	$C_{37}H_{69}O_4$	577.49	577.52	−45.9
	DG (36:2)	$C_{39}H_{71}O_4$	603.55	603.55	−38.4
Negative					
	Palmitoleic acid	$C_{16}H_{29}O_2$	253.22	253.22	14.7
	Palmitic acid	$C_{16}H_{31}O_2$	255.23	255.23	8.5
	Linoleic acid	$C_{18}H_{31}O_2$	279.23	279.23	15.2
	Oleic acid	$C_{18}H_{33}O_2$	281.24	281.25	28.7

Comparison of groups

Figure 3 shows TOF-SIMS reference spectra of corticosterone and 11-dehydrocorticosterone (Fig. 3a and b), a TOF-SIMS spectrum from an analysis of mouse adipose tissue (Fig. 3c) and a multivariate analysis of TOF-SIMS spectra of adipose tissue from TG mice expressing the FOXC2 gene and wild-type controls. The spectra of the glucocorticoids (GC) show well defined peaks ($M+H^+$) at *m/z* 345 and 347. These peaks are also readily defined in the TOF-SIMS analysis of adipose tissue (Fig. 3c). Of the peaks found in the spectra of tissue samples, 47 different peaks were used for multivariate analysis. GC and DG were among the peaks that showed a high rating in explaining the difference between the cytochemistry of adipose tissue in these animals (Fig. 3d).

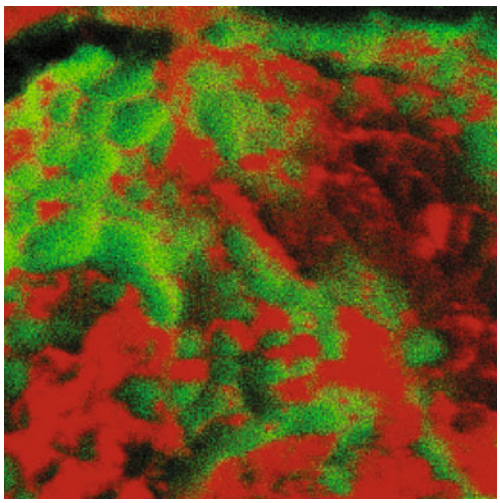

Fig. 4 TOF-SIMS ion image of high pressure frozen, freeze-fractured and freeze-dried mouse adipose tissue showing the distribution of sodium ions (*m/z* 23, green) and potassium ions (*m/z* 39, red) denoting the extracellular and intracellular spaces

The TOF-SIMS analytes found in adipose tissue from tissue wild-type and TG mice are shown in Table 1, together with their secondary ion and accuracy of measurement (ppm).

Extracellular and intracellular areas of adipose tissue can be defined based on their Na and K content (Fig. 4) and this definition can be utilized in the TOF-SIMS analysis of organic compounds. Data from intensity measurements on the high pressure frozen mouse adipose tissue is presented in Tables 2 and 3. Differences in peak intensities between TG and wild-type tissue biopsies in selected intracellular ROI are shown in Table 2. All measured intensities are normalized to the area of the analyzed region and given as means±S.E.M. Differences in the content of DG species are significant ($p<0.001$) for DG (32:0), for DG (34:1; $p<0.0005$) and for DG (36:2; $p<0.05$). The adipose tissue of TG animals shows six to ten times lower peak intensity than that of the wild-type animals.

The peak intensities for the fatty acids are all significantly lower for the TG tissue than wild-type tissue, with $p<0.0005$ for palmitoleic acid C16:1, $p<0.005$ for palmitic acid C16:0, $p<0.001$ for linoleic acid C18:2, and $p<0.0005$ for oleic acid C18:1.

The adipose tissue of TG animals shows two to three times lower peak intensities of 11-dehydrocorticosterone ($p<0.001$) and corticosterone ($p<0.005$) than that of the wild-type animals. The ratio of corticosterone/dehydrocorticosterone is higher (1.7) in wild-type animals, indicating a higher activity of 11-HSD type 1 enzyme in the adipose tissue of these animals than in TG animals (ratio 1.4).

Table 3 shows differences in peak intensities between TG and wild-type mouse adipose tissue biopsies in selected extracellular ROI. All measured intensities are normalized to the area of the selected regions found in the ion image. The extracellular space of TG adipose tissue shows six to seven times lower peak intensities for 11-dehydrocorticosterone ($p<0.001$) and corticosterone ($p<0.005$) than the corresponding compartment of the wild-type tissue. The ratio of corticoste-

Table 2 Differences in peak intensities between TG and wild-type WAT mouse tissue biopsies in intracellular regions of interest

Designation	*m/z*	PI, TG	S.E.M.	PI, WT	S.E.M	*p*
Palmitoleic acid	253.2	22,182	2,458	39,567	2,036	2.25E−005
Palmitic acid	255.2	92,638	8,353	132,065	7,676	2.26E−003
Linoleic acid	279.2	12,672	2,058	52,725	3,671	5.91E−008
Oleic acid	281.2	40,723	6,344	82,769	4,816	3.62E−005
11-Dehydrocorticosterone	345.2	40	7	85	8	5.15E−004
Corticosterone	347.2	57	10	145	15	1.61E−004
DG(32:0)	551.5	25,403	4,467	52,855	5,221	9.52E−004
DG(34:1)	577.5	12,206	941	26,520	2,406	1.42E−004
DG (36:2)	603.5	3,659	1,006	6,603	671	2.87E−002

All measured intensities are normalized to the area of the selected cellular region (TG $n=9$, WT $n=10$)

rone/dehydrocorticosterone is not significantly different between the extracellular compartments of the adipose tissue of the TG and wild-type animals (1.86 and 1.88). Comparison with the ratios of the GC in the intracellular compartment suggests that corticosterone is dehydrogenated in adipocytes of the TG animal.

Differences between the different DG species are also significant with $p<0.005$, $p<0.001$ and $p<0.005$ respectively and the TG tissue shows five to eight times lower peak intensity than the wild-type tissue.

Comparison between peak intensities in intracellular and extracellular ROI in TG adipose show that the mean peak intensities for 11-dehydrocorticosterone and corticosterone are significantly higher in the intracellular areas ($p<0.01$ and $p<0.05$, respectively).

Comparison between peak intensities of GC in intracellular and extracellular ROI in wild-type mouse adipose tissue shows no significant difference between the compartments.

Histopathology

Figure 5 shows a cryosection of a muscle biopsy taken from a child 5 months of age, suffering from infantile reversible cytochrome c oxidase deficiency myopathy. A light microscopy image of a cryosection stained with Sudan black (Fig. 5a), is shown together with TOF-SIMS images showing the distribution of cholesterol (Fig. 5b) and DG (Fig. 5c). The light microscopy image reveals lipid accumulation in cytoplasmic vesicles of a diameter of 1–3 μm indicated by arrows. Cells containing lipid accumulation were analyzed with TOF-SIMS in order to investigate the identity of the lipids. ROI spectra from the darkly stained regions indicated in the Sudan black staining showed the presence of cholesterol (*m/z* 369) and diacylglycerol (*m/z* 551 and 577). Imaging the distribution of cholesterol signal and diacylglycerol signal shows even distribution of cholesterol in the muscle cells, and specific localization of DG corresponding with the lipid accumulating vesicles detected by Sudan black staining (Fig. 5a).

Discussion

Cytochemistry

The possibility, by TOF-SIMS, to localize lipids with <1 μm lateral resolution in intact tissue is illustrated in Figs. 1 and 2. The analysis of the otherwise difficult to study chondocytes in the tracheal wall is of importance for understanding cartilage repair strategies [12]. The DG found in chondrocytes is probably a fragment of triacylglycerol that loses one fatty acid upon ionization [13]. The conclusion is that chondrocytes store lipids in the same manner as adipocytes do [13]. This information has not been found in the literature, suggesting that lipid storing in chondrocytes is described here for the first time and this information would have been difficult to detect with a conventional probe-based cytochemical technique.

Imaging of GC in the adrenal gland is another example of where probe-free detection of lipids gives a unique analysis of the corticosterone secondary ion signal (*m/z* 347, Fig. 2c). Adrenal corticosteroids enter the brain and

Table 3 Differences in peak intensities between extracellular ROIs in TG and wild-type WAT mouse adipose tissue

Designation	*m/z*	PI, TG	S.E.M	PI, WT	S.E.M	*p*
11-Dehydrocorticosterone	345.2	15	3	98	16	5.96E−004
Corticosterone	347.2	28	5	172	25	1.99E−004
DG(32:0)	551.5	5,052	1,490	27,070	4,709	1.01E−003
DG(34:1)	577.5	3,322	480	23,119	4,089	8.91E−004
DG (36:2)	603.5	1,517	343	12,026	2,254	1.13E−003

All measured intensities are normalized to the area of the selected cellular region ($n=10$)

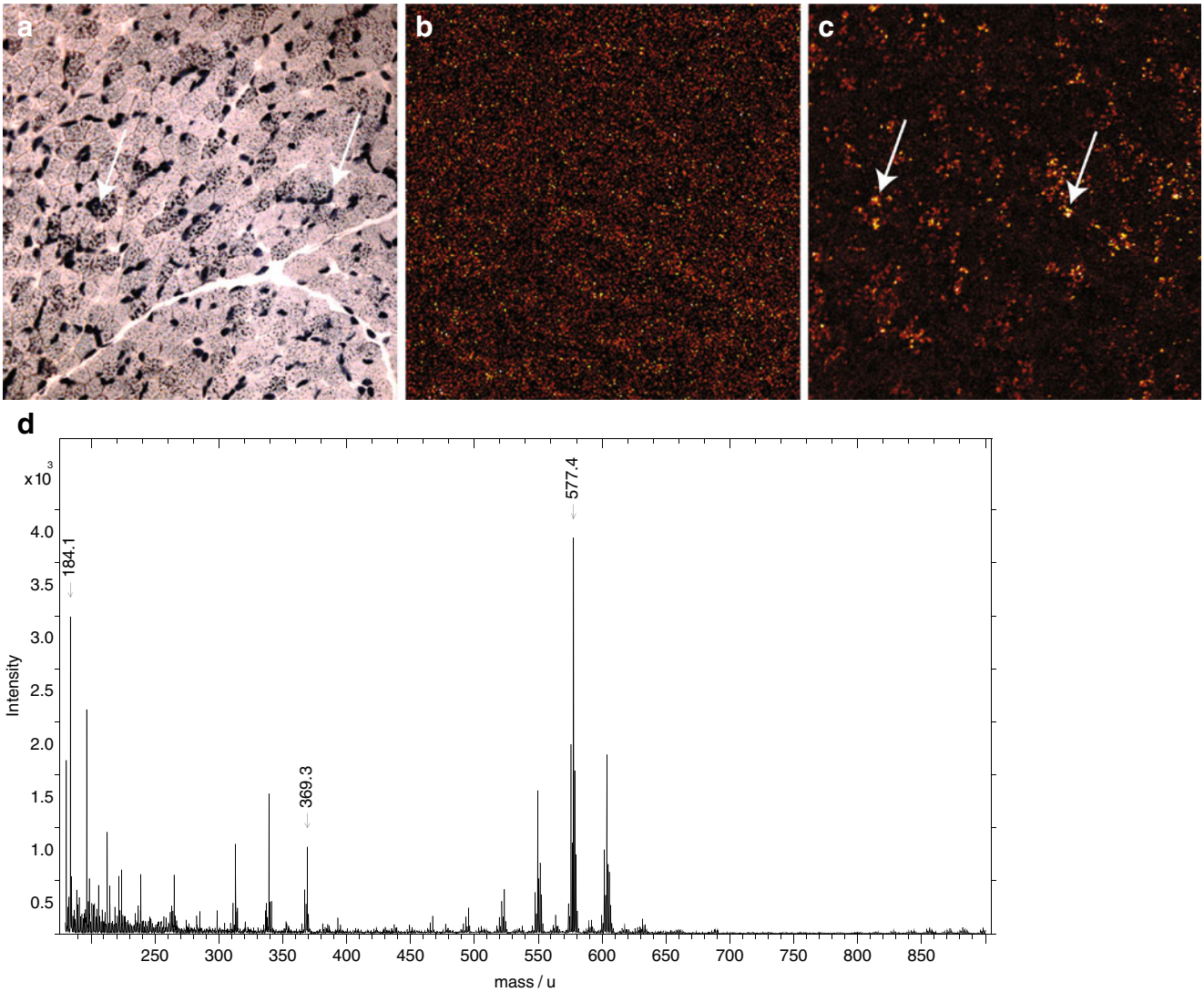

Fig. 5 Cryostat section of a human muscle biopsy. **a** Light microscopy image of section stained with Sudan black. Image size 300×300 μm. **b** TOF-SIMS ion image showing the distribution of cholesterol (*m*/*z* 369). **c** TOF-SIMS ion image showing the distribution of diacylglycerol (*m*/*z* 551 and 577)

exert markedly diverse effects, such as the stress response of target neural cells. Insights into GS levels in tissue can give insights into many different cytochemical processes.

Comparison of groups

The finding that a steroid hormone, like corticosterone, can be detected by TOF-SIMS (Fig. 2) was further exploited in studies of adipose tissue, where GC are thought to be locally produced in the tissue and may affect the differentiation of adipocytes [14–16]. The issue to be solved is then whether or not the TOF-SIMS signal might be treated as a quantitative measurement. Assuming that the microenvironment (matrix) of the tissue samples is similar from one sample to the next, one can certainly get relative quantification by comparing groups of animals. The experimental design, with appropriate control groups, offers the possibility of comparing TOF-SIMS data from the same area in different samples thus "normalizing" the experiment group to the control group. In this context, we also use the advantage of measurements in ROI meaning that cell compartments may be selected and the spectra of the selected regions can be compared without interference from other parts of the image.

The presented data indicate the possibility of analyzing molecules present in small quantities, like steroid hormones, in an environment of complex macromolecules and high salt concentrations. In the wild-type animal a high level of GC is found both in EC and IC, indicating a high blood level of GC maintained by production of hormone in the cortex of the adrenal gland. The steroids penetrate the cell membranes

resulting in a high level of GC in the adipocytes. The ratio of corticosterone/dehydrocorticosterone is similar in the EC and IC departments of the adipose tissue of wild-type animals, indicating a limited local influence of GC-converting enzymes in the adipose tissue of these animals.

The intracellular levels of GC in TG animals are higher than the EC levels indicating a local production of GCs by GC-converting enzymes in these cells.

The differences in fatty acid content and content of DG in the adipose tissue of FOXC2 TG and wild-type mice may be expected from the functional differences between the cells. The FOXC2 cells have a high metabolic activity and the adipose tissue of the wild-type mice is rich in stored lipids. The results thus support the assumption that comparison of quantitative data between adipose tissue of different animal strains is possible.

Histopathology

Analysis of histopathological samples by high-resolution TOF-SIMS as shown in Fig. 5 has the important property of imaging the distribution of different lipids in relation to the pathological structure shown by LM images. Analysis of the same sample with other methods, like cutting out parts of the section and analyzing by for example HPLC-MS or ESI-MS will not provide the information about the different localisation of cholesterol and DG as shown by ROI analysis by TOF-SIMS. Imaging MALDI is an alternative technique here but would not as easily ionize cholesterol or provide the spatial resolution that TOF-SIMS does [17]. Due to the large amount of DGs, a fragment of triacylglycerol, detected in the pathological structure of the muscle cells, reversible cytochrome c oxidase deficiency myopathy [9] is suggested to result in storage of triglycerides in muscle cells (Fig. 5).

The advantage of using high-resolution imaging TOF-SIMS in medical research is the possibility to analyze intact tissue and localize target molecules in cells and different tissue compartments. When compared to immunocytochemistry, the TOF-SIMS analysis is probe-free and thus not dependent on penetration of reagents into the sample and also independent of probe reactivity such as cross-reactivity or background staining. When compared to analysis of bulk preparation by extraction and purification, the TOF-SIMS method is quantitative and allows analysis of target molecules in different tissue compartments.

References

1. Kollmer F (2004) Cluster primary bombardment of organic materials. Appl Surf Sci 231:153–158
2. Nygren H, Malmberg P (2007) High resolution imaging by organic secondary ion mass spectrometry. Trends Biotechnol 25:499–504
3. Chughtai K, Heeren RM (2010) Mass spectrometric imaging for biomedical tissue analysis. Chem Rev 110:3237–3277
4. Benabdellah F, Seyer A, Quinton L, Touboul D, Brunelle A, Laprévote O (2010) Mass spectrometry imaging of rat brain sections: nanomolar sensitivity with MALDI versus nanometer resolution by TOF-SIMS. Anal Bioanal Chem 396:151–162
5. Nygren H, Borner K, Hagenhoff B, Malmberg P, Mansson J-E (2005) Localization of cholesterol, phosphocholine and galactosylceramide in rat cerebellar cortex with imaging TOF-SIMS equipped with a bismuth cluster ion source. Biochim Biophys Acta 1737:102–110
6. Nygren H, Malmberg P, Kriegeskotte C, Arlinghaus HF (2004) Bioimaging TOF-SIMS: localization of cholesterol in rat kidney sections. FEBS Lett 566:291–293
7. Cederberg A, Gronning LM, Ahren B, Tasken K, Carlsson P, Enerback S (2001) FOXC2 is a winged helix gene that counteracts obesity, hypertriglyceridemia, and diet-induced insulin resistance. Cell 106:563–573
8. Studer D, Graber W, Al-Amoudi A, Eggli P (2001) A new approach for cryofixation by high-pressure freezing. J Microsc 203:285–294
9. Horvath R, Kemp JP, Tuppen HA, Hudson G, Oldfors A, Marie SK, Moslemi AR, Servidei S, Holme E, Shanske S, Kollberg G, Jayakar P, Pyle A, Marks HM, Holinski-Feder E, Scavina M, Walter MC, Coku J, Gunther-Scholz A, Smith PM, McFarland R, Chrzanowska-Lightowlers ZM, Lightowlers RN, Hirano M, Lochmuller H, Taylor RW, Chinnery PF, Tulinius M, DiMauro S (2009) Molecular basis of infantile reversible cytochrome c oxidase deficiency myopathy. Brain 132:3165–3174
10. Kollmer F (2004) Cluster primary ion bombardment of organic materials. Appl Surf Sci 231–2:153–158
11. Sodhi RN (2004) Time-of-flight secondary ion mass spectrometry (TOF-SIMS): versatility in chemical and imaging surface analysis. Analyst 129:483–487
12. Lafont JE (2010) Lack of oxygen in articular cartilage: consequences for chondrocyte biology. Int J Exp Pathol 91:99–106
13. Malmberg P, Nygren H, Richter K, Chen Y, Dangardt F, Friberg P, Magnusson Y (2007) Imaging of lipids in human adipose tissue by cluster ion TOF-SIMS. Microsc Res Tech 70:828–835
14. Bronnegard M, Arner P, Hellström L, Akner G, Gustafsson J (1990) Glucocorticoid receptor messenger RNA in different in different regions of human adipose tissue. Endocrinology 127:1689–1696
15. Rask E, Olsson T, Söderberg S, Andrew R, Livingstone D, Johnson O, Walker B (2001) Tissue-specific dysregulation of cortisol metabolism in human obesity. J Clin Endocrinol Metab 86:1418–1421
16. Bujalska I, Gathercole L, Tomlinson J, Darimont C, Ermolieff J, Fanjul A, Rejto P, Stewart P (2008) A novel selective 11beta-HSD type 1 inhibitor prevents human adipogenesis. J Endrocrinology 197:297–307
17. Murphy RC, Hankin JA, Barkley RM (2009) Imaging of lipid species by MALDI mass spectrometry. J Lipid Res 50(Suppl):S317–S322